Optical Materials 58 (2016) 18–23

Contents lists available at ScienceDirect

Optical Materials

journal homepage: www.elsevier.com/locate/optmat

Polymer-based composite with outstanding mechanically tunable refractive index

Nasser Mohamed-Noriega [a, *], Moisés Hinojosa [a], Virgilio González [a], Sandra. E. Rodil [b]

[a] Universidad Autónoma de Nuevo León, Facultad de Ingeniería Mecánica y Eléctrica, Av. Universidad s/n, Cd. Universitaria, San Nicolás de los Garza 66451, Mexico

[b] Universidad Nacional Autónoma de México, Instituto de Investigación en Materiales, Circuito exterior s/n, Cd. Universitaria, México D.F. 04510, Mexico

ARTICLE INFO

Article history:
Received 1 March 2016
Received in revised form
17 March 2016
Accepted 19 March 2016
Available online 13 May 2016

Keywords:
Composite materials
RI
Mechanically tunable
Photoelasticity

ABSTRACT

A composite with high visible light transmittance, mechanically tunable refractive index (RI) and rubber-like mechanical properties, based on poly(dimethylsiloxane) (PDMS) and barium titanate nanoparticles (BT) was prepared on three steps. First, BT nanoparticles were obtained by high-energy milling. Second, the nanoparticles were embedded in PDMS by in-situ polymerization; the BT content was varied up to 1.0 wt% (0.17 vol%). Finally, ~0.5 mm membranes were prepared by solvent casting. The effect of the BT concentration was examined. Powder XRD and Raman spectroscopy revealed a tetragonal crystal structure for the nanoparticles. SEM images confirmed a mean particle size of ~64 nm and together with EDX mappings showed a moderate dispersion of the nanoparticles in some membranes, whereas other exhibited agglomerates at the surface. The normal transmittance of the membranes was measured with a spectroscopic ellipsometer while they were stretched in-situ at different percentages. The RI variations as a function of strain were calculated from the transmittance spectra. The results exhibit surprising variations in the RI, up to ~5 times higher than those associated to PDMS alone, implying that the presence of BT significantly influences the optical response of the PDMS when stretched. However, the response is neither linear nor well understood; further studies must be performed to clarify this new interaction.

1. Introduction

The impact of materials with tailored optical properties is real and massive, as can be appreciated in the telecommunication revolution triggered by optical fiber; materials with the capability to bend light around them or confine it to a specific region of space [1–3] or prevent light propagation in certain directions [4,5] or at certain frequencies [6–8] are only possible if the optical properties can be controlled at will. The last implies the modification of the light-matter interaction; this interaction is mainly defined by the RI (n) which in turn is defined by the electric (electric permittivity $-\varepsilon_r$) and magnetic (magnetic permittivity $-\mu_r$) response of the material ($n=\sqrt{\varepsilon_r\mu_r}$). It is known that the RI of a material can be "adjusted" by simply changing its composition (by either doping or mixing different materials, like in a composite) [9–12]; however, this change is a passive change, since it is only defined by the RI and the volume fraction of each of the different constituents of the material (the last is described by the "Effective Medium Approximation" – EMA), without any further interaction beyond the mixing, in contrast to changes in the RI achieved as a result of an external stimulus, such as chemical [13,14], thermal [15], photonic [16,17], magnetic [18,19], electric [20,21] or mechanical [22,23]. Moreover, the changes result from an external stimulus may be reversible in most cases, leading to materials with tunable RI; such materials have drawn the attention of scientist and industry due to their potential range of applications such as adjustable lenses, waveguides, optical filters, optical shutters/switches and sensors, among others.

Leaving aside stress-induced-birefringence, few reports are found in literature about the photoelastic properties of materials, especially when designing devices/materials with tunable RI, like adjustable lenses; other stimulus like electric and chemical are preferred. Perhaps, the reason lies on the magnitude of the RI variations achieved by a mechanical stimulus, compare to other stimulus. All materials present a variation on the RI as a response to a mechanicals stimulus, but the variations obtained are commonly small for polymers [24–27] and even smaller for harder materials

* Corresponding author.
E-mail addresses: nmn270382@gmail.com, nasser.mohamednr@uanl.edu.mx (N. Mohamed-Noriega).

http://dx.doi.org/10.1016/j.optmat.2016.03.039
0925-3467/

like glass or inorganic crystals [28–31]; however, for some applications or environments a mechanical stimulus is the only suitable stimulus.

Polymer-based composites incite great interest when designing materials with tunable RI due to the variety of properties that could be achieved when fillers are incorporated [10], especially of inorganic nature; polymers offer a flexible, transparent and easily processable matrix, while the fillers provide the active or functional element. Thus, this paper proposes a composite material with mechanically tunable RI, composed of a transparent polymer matrix, with embedded piezoelectric nanoparticles as active filler. It is expected that the piezoelectric nanoparticles polarize electrically as a consequence of the applied mechanical stimulus and that such polarization affects the local field of the polymer [32] provoking a change in its electric permittivity and subsequently in the RI; considering the mechanical properties of the polymer matrix, a reversible and tunable change in the RI is expected. It is not in the knowledge of the authors that such kind of interaction has been previously studied, thus the aim of this work is to evaluate the feasibility of such material.

PDMS is a popular elastomer for its clarity, flexibility and chemical resistance, while BT is well known for its piezoelectric properties, which have been studied at the macroscale [33], microscale [34,35] and nanoscale [36–40]. Nevertheless, the incorporation of any kind of filler into a polymer matrix may cause significant light scattering, diminishing the transparency of the composite, if the particle size is not considerably smaller than the wavelength of the incident light (for spherical particles $2r < \lambda/10$); thus, in the visible range, a particle size of around 50 nm assures little scattering as long as the particles are homogeneously dispersed, as reported by several authors [10,41–43]. However, it is also known that as the particle size of piezoelectric materials decreases, the electric permittivity (which is associated to the piezoelectric properties) reduces until it reaches a “critical size” where the piezoelectric properties are lost [44,45]. Recent studies on BT have shown that depending on the synthesis method, the “critical size” may vary between 3 nm and 100 nm, with a major incidence around 20 nm [39,46–51]; the “critical size” is associated with the stabilization at room-temperature of the paraelectric cubic polymorph, instead of the tetragonal crystal structures which is normally stable up to 120 °C in bulk [52]. Because of that, it is essential to ensure the tetragonality of the BT nanoparticles.

To confirm the proposed interaction between the polymer matrix and the piezoelectric nanoparticles, we measured the normal transmittance and calculated the RI of thick membranes made of a composite based on poly(dimethylsiloxane) (PDMS) and different amounts of barium titanate nanoparticles (BT), while they were in-situ bi-directionally stretched at different percentages.

2. Experimental

2.1. Materials

Barium titanate was provided by Sigma-Aldrich (CAS: 12047-27-7) as a powder with particle size smaller than 2 μm (purity 99.9%); it was used as received without purification. Poly(-dimethylsiloxane) was purchased from Dow Corning (SYLGARD 184) as a two-component kit, composed of a polymer base and a curing agent; mixed at a 10:1 ratio and preferably heat cured. Chloroform was obtained from ACS Chemicals and used as a solvent and a dispersant.

2.2. Nanoparticles preparation

A high-energy mill was used for 30 min to pulverize the BT powder and obtain a particle size of ~60 nm. This particle size was chosen to avoid the “size-effect” of ferroelectrics and to minimize the light scattering at the visible range.

2.3. Nanocomposites preparation

The BT content was varied up to 1.0 wt% (0.17 vol%) (Table 1). First, the BT nanoparticles were dispersed in the polymer base and sonicated for ~30 min. Subsequently, chloroform was added to the dispersion and sonicated for another 5 h; afterwards, the dispersions were kept overnight to improve the wetting of the particles. Next day, the dispersions were placed into a water bath at 50 °C and mechanically mixed for 10 h (curing-time required in the PDMS specifications), while the curing agent was added to initiate the polymerization. Finally, ~0.5 mm membranes were prepared by pouring the PDMS-chloroform solution in a Petri-dish and placing it in a vacuum furnace at 50 °C for 20 h to extract the solvent and air of the membranes. The thickness of the membranes was chosen to assure a self-holding membrane (no substrate needed).

2.4. Characterization

The crystal structure of the BT nanoparticles was determined by X-ray diffraction using Cu Kα radiation and by Raman spectroscopy with a 514 nm laser. SEM was used to determine the mean particle size and to qualitatively evaluate the distribution of the particle in the membranes (with the aid of EDX mappings). The RI was calculated from measurements of normal transmittance (in a spectroscopic ellipsometer), while the membranes were in-situ stretched at different percentages (Strain = 0%–24%); the material was modeled with the Cauchy model [53] and the transmittance spectra with the Fresnel equation. In order to in-situ stretch the membranes and evaluate the evolution of the RI as a function of deformation, a mechanical device capable of producing “radial stress” on the membranes was designed and fabricated (Fig. S3); the device assembles to the ellipsometer.

3. Results and discussion

3.1. Characterization of nanoparticles

Fig. 1 shows the particle size distributions of BT powders as-received and after 30 min of milling. Normality tests performed on the data indicated a D50 diameter of ~532 nm and ~64 nm for the as-received and milled powders respectively; representative SEM images are shown in Fig. S1. Considering the preparation method, the particle size distribution of the milled powder is moderately narrow; however, the presence of aggregates could not be avoided.

Since the tetragonal structure is the desired polymorph of BT, it was essential to confirm the crystal structure after milling. Fig. 2 shows the diffractograms of the as-received and milled powders. The crystal structures were assigned to tetragonal BT, as shown by the reference; the peaks that do not correspond to tetragonal BT are marked with a black dot and belong to $BaCO_3$ produced by the decomposition of BT when exposed to environmental CO_2 [54,55]. Additionally, the inset in Fig. 2 shows a magnification of the diffractograms in the 2θ region between 40° and 50°, usually used to distinguish between the cubic and tetragonal structure of BT. Typically, the discrimination between cubic and tetragonal arises from the splitting of the peak associated to the (200) plane of the cubic phase, into the two peaks associated to the (200)/(002) planes of the tetragonal phase. However, the splitting may be masked by the broadening of the peaks as the crystal size decreases in the nanoscale; nevertheless, Raman spectroscopy can distinguish

Table 1
Design of experiments.

	Sample M0	Sample M1	Sample M2	Sample M3	Sample M4	Sample M5
wt% BT	0.00%	0.05%	0.25%	0.50%	0.75%	1.0%
wt% PDMS (Base)	90.90%	90.86%	90.68%	90.45%	90.22%	90.00%
wt% PDMS (Curing Agent)	9.10%	9.08%	9.06%	9.04%	9.02%	9.00%

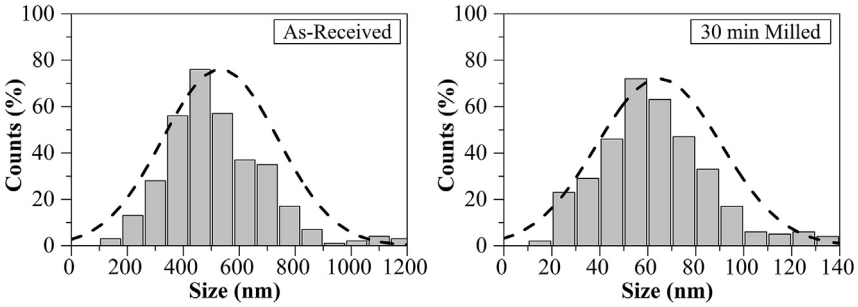

Fig. 1. Particle size distributions of BT powders as-received (left) and after 30 min of milling (right); a dashed normal curve was drawn as an aid to the observer.

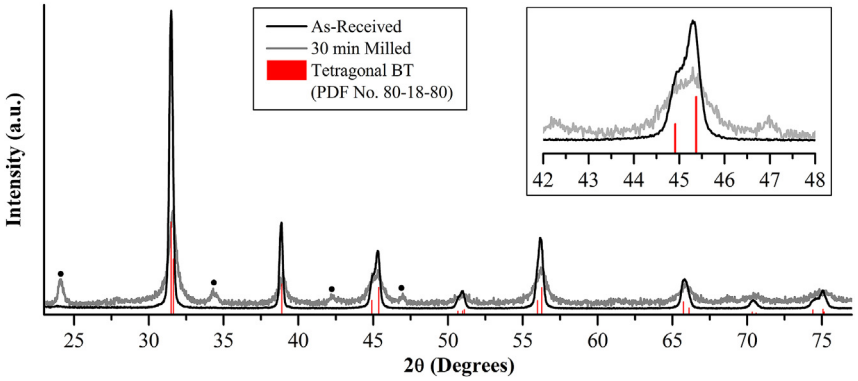

Fig. 2. Diffractograms of BT powders as received (black) and after 30 min of milling (gray), with a magnification (inset) in the region corresponding to the (002)/(200) diffraction planes. As a reference, the relative peak intensities for tetragonal BT (PDF No. 80-18-80) are shown (red); the black dots correspond to $BaCO_3$ peaks. (For interpretation of the references to colour in this figure legend, the reader is referred to the web version of this article.)

between the cubic and tetragonal structure. Fig. 3 shows the Raman spectrums of the as-received and milled powders. The peaks around 180 cm^{-1}, 307 cm^{-1}, 525 cm^{-1} and 715 cm^{-1} are characteristic of the tetragonal structure [46,56,57]. From the diffractograms and the Raman spectrums is evident that the milled powder has a predominantly tetragonal crystal structure.

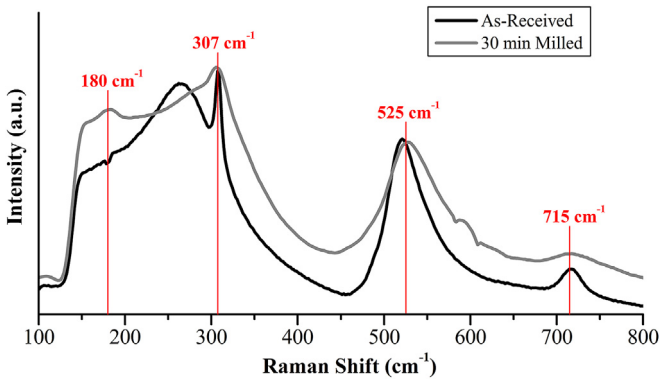

Fig. 3. Raman spectrums of BT powders as-received (black) and after 30 min of milling (gray); the representative bands for tetragonal BT (180 cm^{-1}, 307 cm^{-1}, 525 cm^{-1} and 715 cm^{-1}) are shown with a red line. (For interpretation of the references to colour in this figure legend, the reader is referred to the web version of this article.)

3.2. Characterization of nanocomposites

Fig. 4 shows photographs of the membranes with different BT contents. Given that the PDMS and the BT are transparent to visible light, the loose in transparency is due to scattering; most probably caused by the presence of large aggregates. SEM images and EDX mappings (Ba and Ti) show the distribution of BT into the PDMS matrix and evidence the presence of aggregates (Fig. S2); the SEM images show the fracture surface of the membranes after they were embrittled with liquid nitrogen and transversally fractured. Sample M1 and M2 show no sign of aggregation, while M3 to M5 show large aggregates (4–15 μm) close to the surface of the membranes. An increasing content of BT and specially the presence of large aggregates close to the surface of the samples M3 to M5 reduce drastically the transparency of the samples. The transmittance spectrum was obtained for each sample at seven strain percentages (0%, 4%, 8%, 12%, 16%, 20% and 24%); Fig. 5 shows the average of each spectrum, where the variation of the normal transmittance is

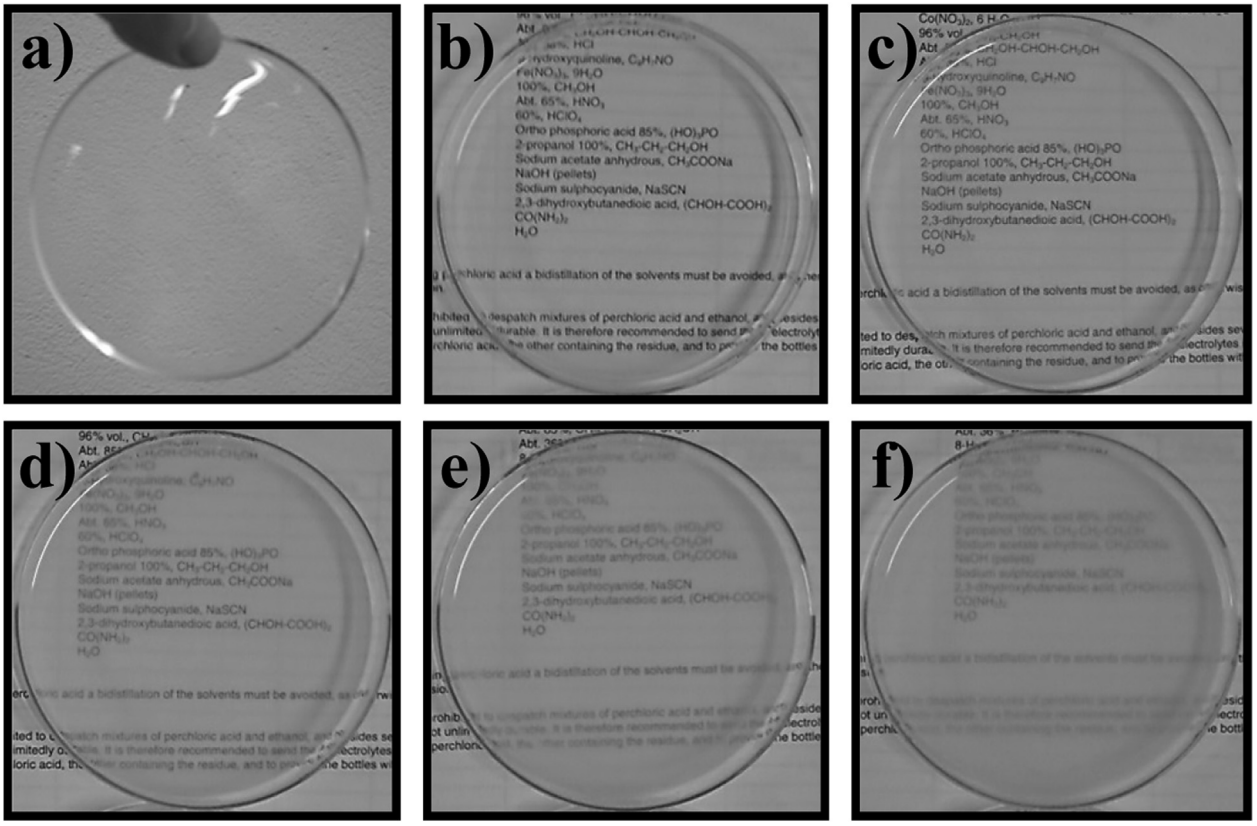

Fig. 4. Photograph of sample M0 = 0.0 BT wt% (a), M1 = 0.05 BT wt% (b), M2 = 0.25 BT wt% (c), M3 = 0.50 BT wt% (d), M4 = 0.75 BT wt% (e) and M5 = 1.0 BT wt% (f).

plotted as a function of the BT content and the strain percentage (strains greater than 24% resulted in the tearing of the membranes). As already mentioned, the transparency losses are mostly due to the presence of large aggregates, while the stretching of the membranes shows little effect on the transmittance; especially at small strains.

The RI of the membranes (dispersion curves) was calculated with the aid of a minimization algorithm (Levenberg-Marquardt) used to fit the transmittance spectrum to the Fresnel equation for normal transmittance, while the membranes were modeled with the Cauchy model; because this model considers a minimal scattering, the samples M3 to M5 were not further analyzed. Table S2 shows the fitting parameter (x^2). To appreciate the effect of the mechanical stimulus on the RI, the difference between the strained and unstrained states are plotted in Fig. 6 ($\Delta n = n_{strain} - n_{unstrain}$) for the samples M0, M1 and M2; the RI at a wavelength of 550 nm was used. It is clear from the graphs that the optical response of the samples cannot be easily described, for neither pure PDMS nor the composites; nevertheless, it is also clear that the presence of BT

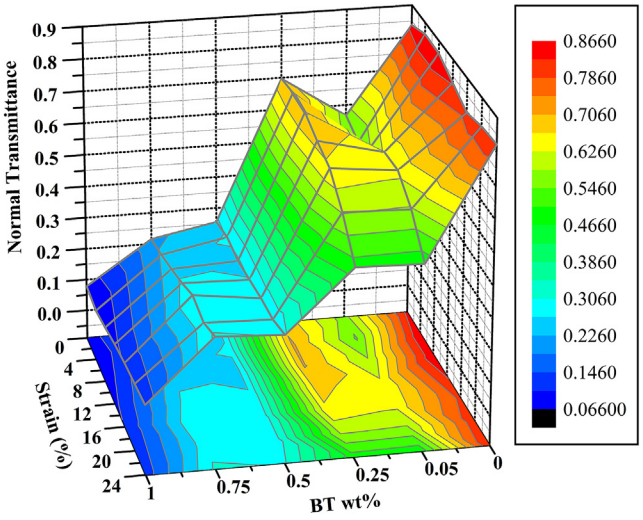

Fig. 5. Variation of the normal transmittance of the membranes as a function of the BT content and the percentage of strain.

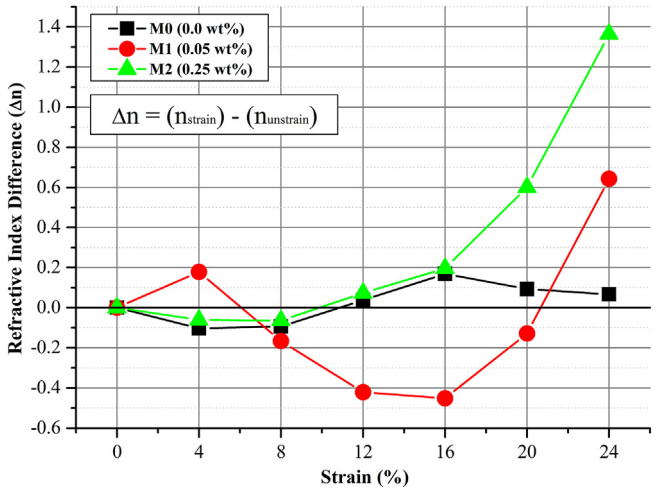

Fig. 6. RI difference (at 550 nm) as a function of strain for samples M0 = 0.0 BT wt%, M1 = 0.05 BT wt% and M2 = 0.25 BT wt%.

nanoparticles significantly changes the optical response of the PDMS. To simplify the comparison and gain an idea of the ability of the material to tune the RI, let us compare the difference between the highest and the lowest value for a particular sample. The difference for sample M0 is 0.2727 and since it is pure PDMS, it is just associated to the photoelastic effect of PDMS [58,59], while for samples M1 and M2 the difference is 1.0944 and 1.4282 respectively. Compared to sample M0, sample M1 and M2 show a variation around 4 and 5 times higher respectively; a colossal change in the RI. Nevertheless, a significant change in the RI of the PDMS should not be expected with such a small amount of BT (less than 0.25 wt%) according the Effective Medium Approximation (EMA), but it is this fact itself what surprises, since it can only be understood if an additional and different interaction between the BT nanoparticles, the PDMS matrix and the mechanical stimulus takes place, rather than just the simple effect of mixing two materials with different RI.

Now, to appreciate the tuning capability of the composites developed in this work it is interesting to compare them with the results obtained by other approaches used to tune the RI. From the different stimuli available to produce a change in the RI, the electric stimulus is one of the most explored, due to its direct interaction with the electric field of light and the variety of materials sensible to it; for example, a liquid crystal cell with one circular electrode working as a lens produces a change of ~0.9 in RI, depending on the input voltage [21]. On the other hand, other research groups obtained variations of ~0.6296 by changing the pH of a solvent [13], ~0.098 via a photoisomerization reaction [16] and ~0.013 as a result of compressing a stacking of layers of two different materials [23]. Another different approach to produce a change in the RI are photonic crystals (PC), which are based on the light-matter interaction, rather than in the stimuli-matter interaction. The classical example is a rigid arrangement of metallic open-rings embedded in a dielectric material, capable of a variation up to 2.5, depending on the frequency of the incident electromagnetic wave (normally in the GHz) [60]. Likewise, some flexible PC consisting of silicon pillars incorporated into an elastomeric matrix achieved a variation of ~1.6 in the RI by stretching the PC [61]; the characteristic distance between the pillars changes and therefore the RI.

This work, proves that the proposed polymer-based composite material with embedded piezoelectric nanoparticles has indeed a mechanically tunable RI, with outstanding large variations. However, as amazing as these results may look, the variations on the RI are neither linear nor well understood and new questions concerning the role of the different components and their interaction have arisen; for instance, the size of nanoparticles (therefore, their piezoelectric properties), but specially the mechanical and optomechanical properties of the polymer matrix, since they are known to be sensible to multiple parameters like the filler content [62], temperature [63] and the nature of the mechanical stimulus [64]. Because of that, a thoughtful rheological characterization of the composites has to be performed, in order to fully understand the mechanical interaction between the nanoparticles and the polymer matrix; together with in-situ creep studies during the measurement of the RI to complement the rheological characterization and to understand the time-dependence of the RI variations. Furthermore, studies near the Tg should be performed to evaluate the temperature-dependence of the optical response.

4. Conclusion

Thick membranes of a novel composite that shows visible light transmittance, mechanically tunable RI and rubber-like mechanical properties were made of PDMS and ~64 nm BT nanoparticles with predominantly tetragonal crystal structure. Ellipsometry results revealed that the presence of BT significantly influences the optical response of the PDMS when stretched; however, the optical response showed not to be proportional to neither the BT content nor the strain. The RI variations for the composites with 0.05 wt% and 0.25 wt% of BT were ~4 and ~5 times larger than for pure PDMS respectively. We believe the change in RI is based on the synergic interaction between the mechanical stimulus, the BT and the PDMS, where the mechanical stimulus polarizes the piezoelectric nanoparticles, which in turn change the electric permittivity of the polymer matrix and finally provoking a change in the RI, modifying the propagation of light through the material. This work opens the possibilities to a new phenomenon and a new way to control light, encouraging us to continue to study and clarify the mechanisms by which the RI changes.

Acknowledgements

The authors would like to thank the UANL and the FIME for the funding. Additionally, the authors would like to thank the Prof. Dr. Miguel J. Yacaman from the UTSA (University of Texas at San Antonio), the Advance Material Division of the IPYCIT (Potosin Institute of Scientific and Technologic Research) and the Faculty of Chemistry and Faculty of Civil Engineering of the Universidad Autónoma de Nuevo Leon for their help during the work.

Appendix A. Supplementary data

Supplementary data related to this article can be found at http://dx.doi.org/10.1016/j.optmat.2016.03.039.

References

[1] T. Baba, Slow light in photonic crystals, Nat. Photonics 2 (2008) 465–473, http://dx.doi.org/10.1038/nphoton.2008.146.
[2] J.D. Joannopoulos, P.R. Villeneuve, S. Fan, Photonic crystals: putting a new twist on light, Nature 386 (1997) 143–149, http://dx.doi.org/10.1038/386143a0.
[3] A. Alù, N. Engheta, Multifrequency optical invisibility cloak with layered plasmonic shells, Phys. Rev. Lett. 100 (2008) 113901, http://dx.doi.org/10.1103/PhysRevLett.100.113901.
[4] N.M. Litchinitser, V.M. Shalaev, Metamaterials: loss as a route to transparency, Nat. Photonics 3 (2009), http://dx.doi.org/10.1038/nphoton.2008.280, 75–75.
[5] N. Liu, H. Liu, S. Zhu, H. Giessen, Stereometamaterials, Nat. Photonics 3 (2009) 157–162, http://dx.doi.org/10.1038/nphoton.2009.4.
[6] S.Y. Lin, J.G. Fleming, D.L. Hetherington, B.K. Smith, R. Biswas, K.M. Ho, et al., A three-dimensional photonic crystal operating at infrared wavelengths, Nature 394 (1998) 251–253, http://dx.doi.org/10.1038/28343.
[7] Y. Huang, Y. Feng, T. Jiang, Electromagnetic cloaking by layered structure of homogeneous isotropic materials, Opt. Express 15 (2007) 11133–11141. http://www.ncbi.nlm.nih.gov/pubmed/19547468.
[8] S. John, A. Blanco, E. Chomski, S. Grabtchak, M. Ibisate, S.W. Leonard, et al., Large-scale synthesis of a silicon photonic crystal with a complete three-dimensional bandgap near 1.5 micrometres, Nature 405 (2000) 437–440, http://dx.doi.org/10.1038/35013024.
[9] S. Kaskel, Functional inorganic nanofillers for transparent polymers, in: VDI Berichte, 2006, pp. 57–60, http://dx.doi.org/10.1039/b608177k.
[10] L.L. Beecroft, C.K. Ober, Nanocomposite materials for optical applications, Chem. Mater 9 (1997) 1302–1317, http://dx.doi.org/10.1021/cm960441a.
[11] T. Hanemann, D.V. Szabó, Polymer-nanoparticle composites: from synthesis to modern applications, Mater. (Basel) 3 (2010) 3468–3517, http://dx.doi.org/10.3390/ma3063468.
[12] W. Caseri, Inorganic nanoparticles as optically effective additives for polymers, Chem. Eng. Commun. 196 (2009) 549–572, http://dx.doi.org/10.1080/00986440802483954.
[13] Y.-J. Lee, P.V. Braun, Tunable inverse opal hydrogel pH sensors, Adv. Mater. 15 (2003) 563–566, http://dx.doi.org/10.1002/adma.200304588.
[14] L. Zhai, A.J. Nolte, R.E. Cohen, M.F. Rubner, pH-gated porosity transitions of polyelectrolyte multilayers in confined geometries and their application as tunable Bragg reflectors, Macromolecules 37 (2004) 6113–6123, http://dx.doi.org/10.1021/ma049593e.
[15] L. Dong, A.K. Agarwal, D.J. Beebe, H. Jiang, Adaptive liquid microlenses activated by stimuli-responsive hydrogels, Nature 442 (2006) 551–554, http://dx.doi.org/10.1038/nature05024.
[16] I. Assaid, D. Bosc, I. Hardy, Improvements of the poly(vinyl cinnamate) photoresponse in order to induce high refractive index variations, J. Phys. Chem. B

108 (2004) 2801–2806, http://dx.doi.org/10.1021/jp0306996.
[17] M.-S. Kim, H. Maruyama, T. Kawai, M. Irie, Refractive index changes of amorphous diarylethenes containing 2, 4-diphenylphenyl substituents, Chem. Mater. 15 (2003) 4539–4543, http://dx.doi.org/10.1021/cm030304v.
[18] H. Yu, G. Zhou, F.S. Chau, S.K. Sinha, Tunable electromagnetically actuated liquid-filled lens, Sens. Actuators A Phys. 167 (2011) 602–607, http://dx.doi.org/10.1016/j.sna.2011.03.005.
[19] Y. Zhao, D. Wu, R.-Q. Lv, Y. Ying, Tunable characteristics and mechanism analysis of the magnetic fluid refractive index with applied magnetic field, IEEE Trans. Magn. 50 (2014) 1–5, http://dx.doi.org/10.1109/TMAG.2014.2310710.
[20] Q. Chen, M.R. Lin, J.E. Lee, Q.M. Zhang, S. Yin, Nanocomposites with very large electro-optic effect and widely tunable refractive index, Appl. Phys. Lett. 89 (2006) 141121, http://dx.doi.org/10.1063/1.2360183.
[21] S. Sato, Liquid crystal lens with focal length variable from negative to positive values, IEEE Photonics Technol. Lett. 18 (2006) 79–81, http://dx.doi.org/10.1109/LPT.2005.860397.
[22] W. Park, J.-B. Lee, Mechanically tunable photonic crystal structure, Appl. Phys. Lett. 85 (2004) 4845, http://dx.doi.org/10.1063/1.1823019.
[23] M. Sandrock, M. Wiggins, J.S. Shirk, H. Tai, A. Ranade, E. Baer, et al., A widely tunable refractive index in a nanolayered photonic material, Appl. Phys. Lett. 84 (2004) 3621, http://dx.doi.org/10.1063/1.1738513.
[24] F. Ay, A. Kocabas, C. Kocabas, A. Aydinli, S. Agan, Prism coupling technique investigation of elasto-optical properties of thin polymer films, J. Appl. Phys. 96 (2004) 7147–7153, http://dx.doi.org/10.1063/1.1812823.
[25] H. Shafiee, A. Tagaya, Y. Koike, Mechanism of generation of photoelastic birefringence in methacrylate polymers for optical devices, J. Polym. Sci. Part B Polym. Phys. 48 (2010) 2029–2037, http://dx.doi.org/10.1002/polb.22082.
[26] D. Kác, I. Turek, N. Tarjányi, I. Martinc, Effect of mechanical stress on optical properties of polydimethylsiloxane, Opt. Mater. (Amst) 36 (2014) 965–970, http://dx.doi.org/10.1016/j.optmat.2013.12.049.
[27] F. Schneider, J. Draheim, R. Kamberger, U. Wallrabe, Process and material properties of polydimethylsiloxane (PDMS) for optical MEMS, Sens. Actuators A Phys. 151 (2009) 95–99, http://dx.doi.org/10.1016/j.sna.2009.01.026.
[28] H. Mueller, Theory of the photoelastic effect of cubic crystals, Phys. Rev. 47 (1935) 947–957, http://dx.doi.org/10.1103/PhysRev.47.947.
[29] G.S. Ranganath, S.R. Rajagopalan, S. Ramaseshan, Photoelastic behaviour of ionic crystals, Radiat. Eff. 4 (1970) 313–318, http://dx.doi.org/10.1080/00337577008242020.
[30] R.W. Dixon, Photoelastic properties of selected materials and their relevance for applications to acoustic light modulators and scanners, J. Appl. Phys. 38 (1967) 5149–5153, http://dx.doi.org/10.1063/1.1709293.
[31] H. Mueller, Theory of photoelasticity in amorphous solids, J. Appl. Phys. 6 (1935) 179–184, http://dx.doi.org/10.1063/1.1745316.
[32] C. Kittel, Introduction to Solid State Physics, 7th ed., John Wiley & Sons, Hoboken, New Jersey, USA, 1996.
[33] L. Qi, B. Lee, P. Badheka, L. Wang, P. Gilmour, W. Samuels, et al., Low-temperature paraelectric–ferroelectric phase transformation in hydrothermal BaTiO particles, Mater. Lett. 59 (2005) 2794–2798, http://dx.doi.org/10.1016/j.matlet.2005.03.068.
[34] Z. Dang, Y. Yu, H. Xu, J. Bai, Study on microstructure and dielectric property of the BaTiO3/epoxy resin composites, Compos. Sci. Technol. 68 (2008) 171–177, http://dx.doi.org/10.1016/j.compscitech.2007.05.021.
[35] H. Pant, M. Patra, A. Verma, S. Vadera, N. Kumar, Study of the dielectric properties of barium titanate–polymer composites, Acta Mater. 54 (2006) 3163–3169, http://dx.doi.org/10.1016/j.actamat.2006.02.031.
[36] T. Michael, S. Trimper, J. Wesselinowa, Size effects on static and dynamic properties of ferroelectric nanoparticles, Phys. Rev. B 76 (2007) 1–7, http://dx.doi.org/10.1103/PhysRevB.76.094107.
[37] G. Arlt, D. Hennings, G. de With, Dielectric properties of fine grained barium titanate ceramics, J. Appl. Phys. 58 (1985) 1619. http://ieeexplore.ieee.org/xpls/abs_all.jsp?arnumber=5077599 (accessed 28.09.10).
[38] H. Xu, L. Gao, Tetragonal nanocrystalline barium titanate powder: preparation, characterization, and dielectric properties, J. Am. Ceram. Soc. 86 (2003) 203–205, http://dx.doi.org/10.1111/j.1151-2916.2003.tb03307.x.
[39] T. Hoshina, H. Kakemoto, T. Tsurumi, S. Wada, M. Yashima, Size and temperature induced phase transition behaviors of barium titanate nanoparticles, J. Appl. Phys. 99 (2006) 054311, http://dx.doi.org/10.1063/1.2179971.
[40] R. Cohen, Nanocapacitors: undead layers breathe new life, Nat. Mater. 8 (2009) 366–368, http://dx.doi.org/10.1038/nmat2435.
[41] M.M. Demir, K. Koynov, Ü. Akbey, C. Bubeck, I. Park, I. Lieberwirth, et al., Optical properties of composites of PMMA and surface-modified zincite nanoparticles, Macromolecules 40 (2007) 1089–1100, http://dx.doi.org/10.1021/ma062184t.
[42] F. Papadimitrakopoulos, P. Wisniecki, D.E. Bhagwagar, Mechanically attrited silicon for high refractive index nanocomposites, Chem. Mater. 9 (1997) 2928–2933, http://dx.doi.org/10.1021/cm970278z.
[43] W. Caseri, Nanocomposites of polymers and metals or semiconductors: Historical background and optical properties, Macromol. Rapid Commun. 21 (2000) 705–722, http://dx.doi.org/10.1002/1521-3927(20000701)21:11<705::AID-MARC705>3.0.CO;2–3.
[44] A.J. Moulson, J.M. Herbert, Electroceramics, 2nd ed., Wiley, Chichester, West Sussex, UK, 2003.
[45] T.M. Shaw, S. Trolier-McKinstry, P.C. McIntyre, The properties of ferroelectric films at small dimensions, Annu. Rev. Mater. Sci. 30 (2000) 263–298.
[46] M. Frey, D. Payne, Grain-size effect on structure and phase transformations for barium titanate, Phys. Rev. B. Condens. Matter 54 (1996) 3158–3168. http://www.ncbi.nlm.nih.gov/pubmed/9986215.
[47] J.E. Spanier, A.M. Kolpak, J.J. Urban, I. Grinberg, L. Ouyang, W.S. Yun, et al., Ferroelectric phase transition in individual single-crystalline BaTiO3 nanowires, Nano Lett. 6 (2006) 735–739, http://dx.doi.org/10.1021/nl052538e.
[48] T. Hoshina, S. Wada, Y. Kuroiwa, T. Tsurumi, Composite structure and size effect of barium titanate nanoparticles, Appl. Phys. Lett. 93 (2008) 192914, http://dx.doi.org/10.1063/1.3027067.
[49] M.B. Smith, K. Page, T. Siegrist, P.L. Redmond, E.C. Walter, R. Seshadri, et al., Crystal structure and the paraelectric-to-ferroelectric phase transition of nanoscale BaTiO3, J. Am. Chem. Soc. 130 (2008) 6955–6963, http://dx.doi.org/10.1021/ja0758436.
[50] T. Hoshina, Size effect of barium titanate: fine particles and ceramics, J. Ceram. Soc. Jpn. 121 (2013) 156–161, http://dx.doi.org/10.2109/jcersj2.121.156.
[51] M. Sendova, B.D. Hosterman, Raman spectroscopic study of the size-dependent order parameter of barium titanate, J. Appl. Phys. 115 (2014), http://dx.doi.org/10.1063/1.4880996.
[52] M.E. Lines, A.M. Glass, Principles and Applications of Ferroelectrics and Related Materials, Oxford University Press, Oxford, UK, 1977.
[53] D. Poelman, P.F. Smet, Methods for the determination of the optical constants of thin films from single transmission measurements: a critical review, J. Phys. D. Appl. Phys. 36 (2003) 1850–1857, http://dx.doi.org/10.1088/0022-3727/36/15/316.
[54] M. Wegmann, L. Watson, A. Hendry, XPS analysis of submicrometer barium titanate powder, J. Am. Ceram. Soc. 87 (2004) 371–377, http://dx.doi.org/10.1111/j.1551-2916.2004.00371.x.
[55] N. Sakurai, V. Bojan, J.J. Stapleton, G.-Y. Yang, C.A. Randall, Y. Mizuno, et al., Surface instability in high surface area complex oxides: BaTiO3 study, Jpn. J. Appl. Phys. 48 (2009) 061404, http://dx.doi.org/10.1143/JJAP.48.061404.
[56] U.A. Joshi, S. Yoon, S. Baik, J.S. Lee, Surfactant-free hydrothermal synthesis of highly tetragonal barium titanate nanowires: a structural investigation, J. Phys. Chem. B 110 (2006) 12249–12256, http://dx.doi.org/10.1021/jp0600110.
[57] A. Shi, W. Yan, Y. Li, K. Huang, Preparation and characterization of nanometer-sized barium titanate powder by complex-precursor method, J. Cent. South Univ. Technol. 15 (2008) 334–338, http://dx.doi.org/10.1007/s11771-008-0063-2.
[58] A. Shtukenberg, Y. Punin, O.B. Kahr, Optically Anomalous Crystals, Springer, 2007.
[59] R.E. Newnham, Properties of Materials – Anisotropy, Symmetry and Structure, Oxford University Press, 2005.
[60] F. Zhang, G. Houzet, E. Lheurette, D. Lippens, M. Chaubet, X. Zhao, Negative-zero-positive metamaterial with omega-type metal inclusions, J. Appl. Phys. 103 (2008) 084312, http://dx.doi.org/10.1063/1.2910831.
[61] W. Park, E. Schonbrun, M. Tinker, Q. Wu, J.-B. Lee, Mechanically tunable nanophotonic devices, Mater. Res. Soc. Symp. Proc. 872 (2005) 123–128, http://dx.doi.org/10.1557/PROC-872-J8.6.
[62] F. Mammeri, E. Le Bourhis, L. Rozes, C. Sanchez, Mechanical properties of hybrid organic–inorganic materials, J. Mater. Chem. 15 (2005) 3787–3811, http://dx.doi.org/10.1039/b507309j.
[63] I.V. Kityk, J. Kasperczyk, Low temperature anomalies in polyvinyl alcohol photopolymers, Polymer 38 (1997) 4803–4806.
[64] R.D. Maksimov, E.Z. Plume, J.O. Jansons, Comparative studies on the mechanical properties of a thermoset polymer in tension and compression, Mech. Compos. Mater. 41 (2005) 425–436, http://dx.doi.org/10.1007/s11029-005-0068-y.